

Co-planar PET/CT for Small Animal Imaging

Juan José Vaquero, *Senior Member, IEEE*, Eduardo Lage, Santiago Redondo, Mónica Abella, Javier Pascau, Javier Sánchez, Esther Vicente, María Luisa Soto-Montenegro, Manuel Desco

Abstract—A small animal PET/CT system based on a common rotating gantry is proposed. The PET detection subsystem is composed of two detector modules based on MLS arrays and four flat panel type PS-PMT. The CT subsystem consists in a micro-focus X-ray tube and a semiconductor X-ray detector. Space for opposed PET detectors and the CT scanner have been allocated on the same plane in such a way that the trans-axial and axial centers are common for both systems. Shielding elements have been placed around the detectors to avoid cross modality contamination. The gantry can rotate 370 degrees to provide complete data sets for the CT image reconstruction algorithm that is based on the cone beam geometry. PET image reconstruction is implemented using FBP (2D and 3D) and OSEM. Sequential acquisition protocols minimize the scan duration, and CT information can be used to implement PET imaging corrections. The coplanar configuration of this system provides intrinsically co-registered data sets, and it is not necessary to reposition the animal to perform any modality imaging, avoiding undesired animal or additional accessories movements. An additional advantage is the compactness of the system that saves space and allows a direct visual monitoring of the animal during the scan.

Index Terms— Gamma detectors, position sensitive photomultiplier tubes, positron emission tomography (PET), small animal imaging, biomedical nuclear imaging.

I. INTRODUCTION

Molecular imaging of small laboratory animals like rats and mice make use of anatomical and functional modalities to provide more accurate results. PET and CT imaging is an useful combination of modalities since CT provides not only anatomical landmarks, but attenuation coefficients of the sample tissue that can be used to implement corrections on the PET image reconstruction process [1].

These multimodality studies are usually done using two different instruments; newer PET and CT systems designed for this purpose are axially aligned in such a way that the sample can be transferred from one system gantry to the other

Manuscript received November 14, 2005. Part of this work is founded by the IM3 network (G03/185 Ministerio de Sanidad), with grants from the Ministerio de Educación y Ciencia, project TEC2004-07052-C02-01, and Ministerio de Industria, Turismo y Comercio project FIT-330101-2004-3. J.J. Vaquero has support from the “Ramón y Cajal” Program, Ministerio de Educación y Ciencia.

J.J. Vaquero is with the Unidad de Medicina y Cirugía Experimental, Hospital GU Gregorio Marañón, Madrid, Spain (corresponding author phone: +34-91-426-5067; fax: +34-91-426-5067; e-mail: juanjo@mce.hggm.es).

E. Lage, S. Redondo, M. Abella, J. Pascau, J. Sánchez, E. Vicente, M.L. Soto-Montenegro and M. Desco are with Unidad de Medicina y Cirugía Experimental, Hospital GU Gregorio Marañón, Madrid, Spain.

automatically, reducing the risk of misalignments. However this kind of solutions, based on two axially displaced and essentially independent imaging systems, increases the acquisition time and doesn't avoid undesired movements of the animal or the auxiliary probes and anesthesia hoses attached to it. A recent development makes use of a unique detector sensitive to both types of radiation, x-ray and 511 keV gamma rays, leaving the animal untouched during the two scans [2-4]

The proposed co-planar PET/CT design is based on a common rotating gantry in which four PET detectors and a small animal CT scanner has been integrated. The acquisition protocol for both imaging modalities is based on a step-and-shoot mode in which the gantry is rotated to the appropriate angle and paused while the data is acquired. The PET and CT data are not acquired simultaneously, however, and the two imaging functions will operate sequentially.

II. SYSTEM DESCRIPTION

A. PET Detectors

The PET system is built around two orthogonal pairs that have been coupled together into two wide, opposed detectors (Fig. 1). This geometry provides a trans-axial field of 80 mm. The detectors have a shield, and a shutter block the x-ray scatter illumination of the scintillator crystals.

These detectors are based on $1.5 \times 1.5 \times 12 \text{ mm}^3$ MLS crystals assembled on a 30×30 matrix with reflector between crystals, optically coupled to a position sensitive photo-multiplier. The readout circuits that pre-process the 64 signals from the 8×8 anodes matrix, plus the trigger signal for coincidence detection and timing, and the high voltage supply are integrated in a three PCBs stack that forms the base attached to the back of the PMT, and the whole assembly is enclosed in a light tight, lead (Pb) shielded aluminum box. The events are digitized using a charge-integrating converter and, in turn, they are screened and histogrammed with a modified center of gravity algorithm that removes from the position calculation those signals with poor signal to noise ratio.

B. X-Ray CT System

The CT system uses a 50kV micro-focus x-ray source with a focal spot size of $35 \mu\text{m}$ (Oxford Instruments XTG5011), a beryllium window and a stationary tungsten anode. The assembly is packaged in a stainless steel container filled with oil, ventilated by air convection generated inside the gantry. A tungsten shutter is attached to the x-ray windows non-obstructing the x-ray cone beam. The shutter is controlled by

the computer in synchronism with the gantry rotation and the frame grabber image integration. It can be left permanently open for fast imaging protocols in which subject dose is not an issue.

C. Flat-panel imager

A digital x-ray image sensor (Hamamatsu C7942) is placed in an orthogonal, opposing plane, conforming a cone-beam geometry. This device integrates in one compact flat panel a CsI scintillator plate, a photodiode array with FET switches, and a signal processor. The projection image intrinsic resolution is 2400x2400 pixels, covering an active area of 120x120 mm. The sensor interfaces with the computer through by means of a digital frame grabber card (PIXCI D2X, Epix Inc., Buffalo Grove, IL). This configuration reaches a transfer rate up to 9 frames per second performing with 4 x 4 binning, 4 frames per second with 2 x 2 binning, and 2 frames per second when no binning is performed. Binning modes are used to implement imaging protocols: high speed (lower resolution) or high spatial resolution (higher dose).

D. Gantry and System Geometry

A computerized system operates the source, gantry, sensor, shutter and frame-grabber sequentially to obtain the projection data set needed to reconstruct the object being scanned. The distance from the x-ray tube to the x-ray detector is 440 mm achieving a magnification factor of 1.6, while the distance between opposite PET detector centers is 140 mm. The system allows movements of the sample in the axial direction to perform whole body studies. Typical studies in CT mode consist of 360, 720 or 1080 views acquired over a 360 degrees gantry rotation span. PET scan parameters such as number of steps or angle per step are also software configurable.

Once the projections have been acquired, sent to the computer and post-processed to correct sensor non-uniformities, different reconstruction algorithms adapted to the specific cone-beam geometry (Grangeat, FDK and SART) have been used to obtain tomographic images. The system is controlled through a multi-processor Linux computer in which both the CT and PET acquisition software are implemented. The PET acquisition electronics consist of a control module where the detectors last dynode signals are pre-processed and the coincident events in opposite detectors are discriminated. The acquisition electronics also contain various analog-to-digital conversion modules, which digitize the anode signals of the detectors when a valid event is detected. These digitized events are transferred to the control computer using a Giga Ethernet interface. The computer processes the channel values to obtain the interaction point on each detector [5, 6] and the energy of the two detected gamma photons. This information is recorded in one or more LIST mode files which serve as input for the reconstruction software.

The effects of the focal spot size and the detector image resolution, assuming that the mechanical geometrical alignments are perfect, are well described in [5, 6].

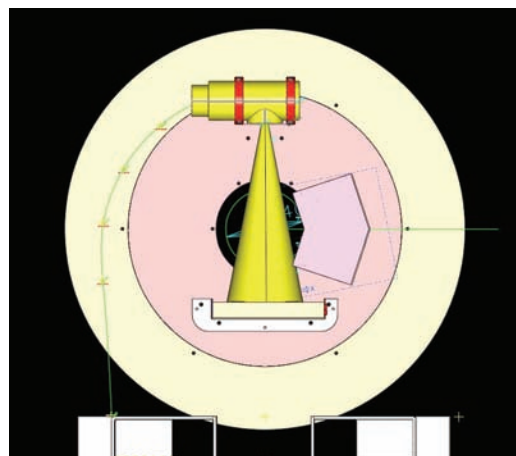


Figure 1: Layout of the PET/CT system showing the X-ray cone projected on the detector and one of the two PET detector boxes on the right of the cone beam.

If ρ_d is the intrinsic resolution of the detector and M is the magnification factor defined by the geometry, the resolution at the FOV center is

$$\sigma_d = \left(\frac{\rho_d}{M} \right)$$

On the other hand, the finite size of the x-ray source focal spot at the FOV center becomes

$$\sigma_f = \left(\rho_f \cdot \frac{M-1}{M} \right)$$

where ρ_f is the nominal focal spot. The resulting image resolution is limited by the geometrical mean of these two factors. The geometric alignment is verified using analytic method based on the identification of elliptical trajectory of two bearing two bearing balls as described on [7].

E. Image Reconstruction

The CT projections are corrected during the process of acquisition before sending them to the reconstruction computer. This correction includes geometrical mis-alignments, with factors calculated as described in [7], and sensor non-uniformities, previously detected on a calibration acquisition. Different reconstruction algorithms adapted to the specific cone-beam geometry (FDK [8], Grangeat [9] and SART [10, 11]) have been implemented. Beam hardening correction and Hounsfield units calibration are also done *a posteriori*. Reconstruction time for a volume of 512³ from 360 projections takes 6 minutes on a standard personal computer. Acceleration techniques for fast reconstructions are been developed for those protocols where high resolution is not a requirement.

For the PET image reconstruction list mode data are aggregated into sinograms, which are the input for analytical reconstruction methods (2D FBP and 3DRP [12]), and statistical (OSEM [13, 14]). Decay, death time, scatter, geometrical effects and crystal sensitivity, are compensated with an experimental correction based on acquisition of flat field-flood. For 2D reconstruction techniques, the corrected sinograms are rebinned using SSRB [15] in order to increase statistics. Filtering in the Fourier domain, transaxial filters

(Hanning, Shepp-Logan, Cosine, Butterworth) and axial smoothing are available to improve reconstructed image quality.

Spatial resolution measurements have been performed using a 0.3 mm diameter ^{22}Na point source (30 μCi), encapsulated in a 1 cm³ in epoxy capsule. The source was placed in the centre of the field-of-view and it was moved radially towards its edge (in central plane). Data were acquired for 10 minutes at each position of the source. They were not corrected for source dimension, positron range, photon non-collinearity or attenuation. 3D data were reconstructed using FBP (Filtered Back-Projection) without smoothing and the profiles through the reconstructed images were fitted with a Gaussian function. The full width at half maximum of the profiles were calculated and plotted against source position.

III. RESULTS

The CT system characteristics are.- cone angle: 22° (alignment errors less than 0.4°); field of view: 75 mm; maximum x-ray energy: 50 kV; tube power: 75 W; flat panel detector pixel size: 50 μm ; area: 120x120 mm²; and resolution: 8 lp/mm, 2400 x 2400 pixels,

The initial CT prototype spatial resolution (FWHM) when operated on its low-resolution mode was 2.44 pl/mm. Fig. 2 shows an image of a 120 μm resolution mouse study, done with a 4x4 binning.



Figure 2: 3D render of a CT bone scan of a mouse, 4x4 binning, 120 μm resolution.

Fig. 3 depicts the dose curves for different x-ray tube kilovoltage and x-ray beam filtering.

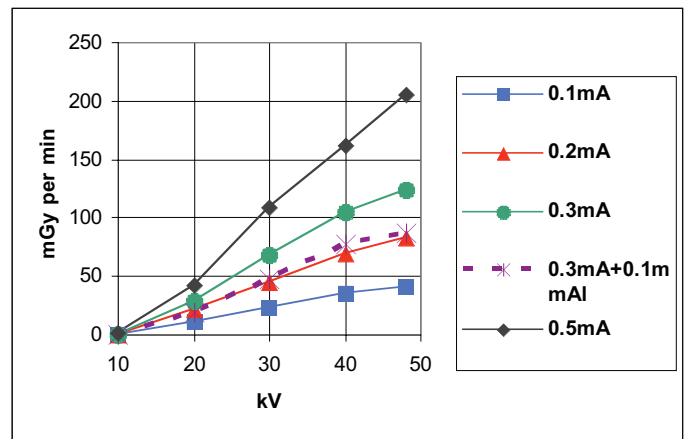


Figure 3: Dose in mGy as a function of kilovoltage and x-ray beam filtering.

The PET system prototype has a 2% central point sensitivity and 1.6 mm FWHM, (FBP) resolution. Apparent mean crystal size on the 511 keV field flood images is 0.6 mm, mean peak-to-valley ratio is better than 8, and intrinsic resolution is 1.5 mm at the central row, and with the energy window wide open. Measured sensitivity for pair of these detectors set in coincidence at 160 mm distance has a CPS of 1%.

Fig. 4 shows the radial, tangential and axial resolution as a function of the source position in the central plane of the FOV; volume resolution is shown in the Fig. 5.

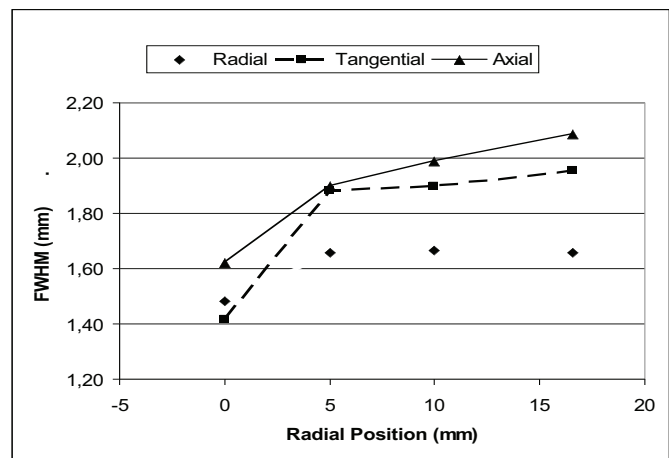


Figure 4: Radial, tangential and axial spatial resolution in central plane.

The sensitivity has been measured using a FDG line source (a linear source in a plastic tube) of 6.64 μCi in 7.3 cm with an energy window of 150-700 KeV. The line source was placed in the center of the FOV along the axial axis of the scanner. The scanner sensitivity was calculated for a pair of detectors taking into account the correction for the branching ratio of 18F (the probability of positron emission for 18F is 96.73 %). The resulting sensitivity in the center of the FOV was 2.8%.

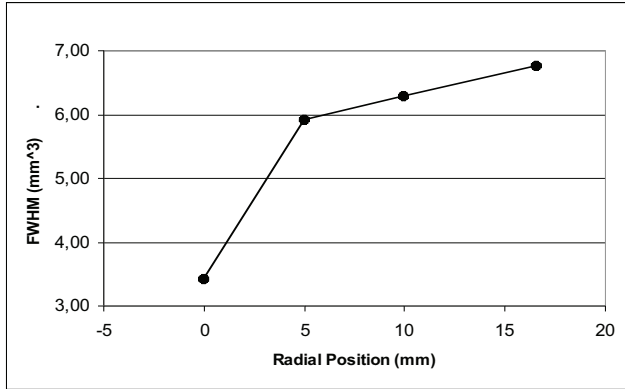


Figure 5: Volume resolution in central plane

Fig. 6 depicts a conventional FDG mouse scan performed with these PET detectors. Scan time was 30 minutes, and during that time the scanner did 45 half-rotations (180 degrees).

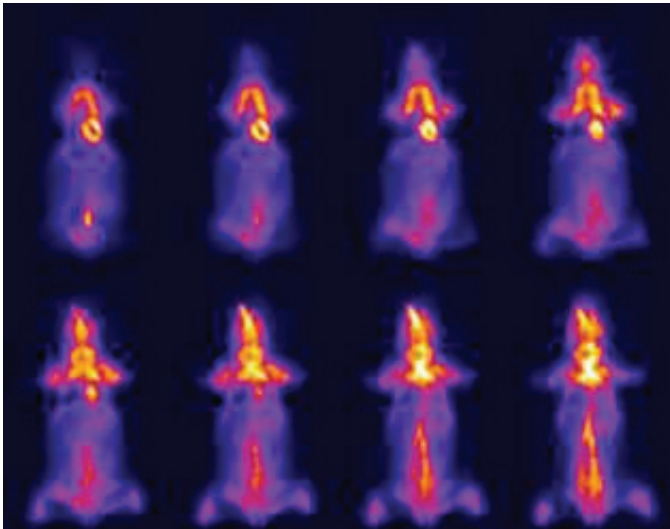


Figure 6: 3D-OSEM coronal images of an FDG full body scan of a 27 gr mouse.

IV. DISCUSSION AND CONCLUSIONS

This work demonstrates the feasibility of a co-planar multimodality system for *in vivo* imaging of small laboratory animals. The physical configuration of this system provides intrinsically co-registered data sets, and it is not necessary to reposition the animal to perform any modality imaging, avoiding undesired animal misalignments. An additional advantage is the compactness of the system that saves space and enables direct visual monitoring of the animal.

Alternative scan methods like step and shoot or helicoidal for both modalities are under development.

ACKNOWLEDGMENT

The authors thank SUINSA Medical Systems Engineering Department for their support with the system design and manufacturing.

REFERENCES

- [1] T. Beyer, P. E. Kinahan, D. W. Townsend, and D. Sashin, "- The use of X-ray CT for attenuation correction of PET data," vol. - 4, pp. - 1577 vol.4, 1994.
- [2] A. Saudi and R. Lecomte, "A novel APD-based detector module for multi-modality PET/SPECT/CT," *IEEE Trans in nuclear science*, vol. 46, pp. 484, 1999.
- [3] R. Fontaine, F. Belanger, J. Cadorette, J. D. Leroux, J. P. Martin, J. B. Michaud, J. F. Pratte, S. Robert, and R. Lecomte, "- Architecture of a dual-modality, high-resolution, fully digital positron emission tomography/computed tomography (PET/CT) scanner for small animal imaging," vol. - 52, pp. - 696, 2005.
- [4] P. Berard, C. M. Pepin, D. Rouleau, J. Cadorette, and R. Lecomte, "- CT acquisition using PET detectors and electronics," vol. - 52, pp. - 637, 2005.
- [5] M. J. Paulus, "High Resolution X-Ray Computed Tomography: An Emerging Tool for Small Animal Cancer Research," *Neoplasia*, vol. 2, pp. 62-70, 2000.
- [6] E. Van de Castele, "Model-based approach for Beam Hardening Correction and Resolution Measurements in Microtomography," in *Faculty Wetenschappen, Department Natuurkunde Antwerpen: University Antwerpen*, 2004.
- [7] F. Noo and R. Clackdoyle, "Analytic method based on identification of ellipse parameters for scanner calibration in cone-beam tomography," *Phys Med Biol.*, vol. 45, pp. 3489-3508, 2000.
- [8] H. Turbell, "Cone-beam reconstruction using filtered backprojection," *Dept. of electrical engineering*, pp. Linköping, Universidad de Linköping, 2001.
- [9] P. Grangeat, *Mathematical framework of cone beam 3D reconstruction via the first derivative of the radon transform*. Germany: Oberwolfach, 1990.
- [10] A. Andersen, "Algebraic reconstruction in CT for limited view," *IEEE Trans. Med. Imag.*, vol. 8, pp. 50-55, 1989.
- [11] A. H. Andersen and A. C. Kak, "Simultaneous algebraic reconstruction technique (SART): a superior implementation of the art algorithm," *Ultrason Imaging* vol. 6, pp. 81-94, 1984.
- [12] P. E. Kinahan and W. Rogers, "Analytic three-dimensional image reconstruction using all detected events," *IEEE Trans in nuclear science*, vol. 36, pp. 964-968, 1990.
- [13] R. E. Carson and K. Lange, "The EM parametric image reconstruction algorithm," *Journal of the Americal Statistical Association*, vol. 389, pp. 20-25, 1985.
- [14] L. A. Shepp and Y. Vardi, "Maximum likelihood estimation for emission tomography," *IEEE Trans Med Imaging*, pp. 113-121, 1982.
- [15] M. E. Daube-Witherspoon and G. M., "Treatment of axial data in three-dimensional PET," *Jour Nucl Med*, vol. 28, 1987.